

**NUMERICAL ANALYSIS OF THE HEAT TRANSFER
AT THE TRANSFERRED ARC ANODE BY USE OF A BLOWING GAS**

Takayuki WATANABE, Takuya HONDA and Atsushi KANZAWA

Department of Chemical Engineering
Tokyo Institute of Technology
O-okayama, Meguro-ku, Tokyo 152, JAPAN

ABSTRACT

The numerical simulation is performed for a transferred arc controlled by a blowing gas. The two-dimensional continuity, x-, r- and θ -momentum, energy and current continuity equations are solved simultaneously with SIMPLER algorithm. The blowing gas is able to control the heat transfer distribution on the transferred anode; the blowing gas is injected from the circumference to the arc with three types of blowing. The vortex flow of the blowing gas is capable of generating the sharp distribution of the heat transfer. The radial inward flow injected at the nozzle exit causes the broad distribution of the heat transfer.

1. INTRODUCTION

The fluid dynamic control by use of a blowing gas is one of plasma-control-techniques. The blowing gas is injected from the circumference to a plasma. The fluid dynamic control of plasma flows is investigated numerically in this paper.

Control of energy flow density of plasma flows is important for various material treatments. High energy density of plasma flows is suitable for plasma cutting because of a demand for the precise cutting-surface, while broad high-temperature region is adequate for plasma spraying, chemical synthesis and production of ultrafine powders.

The fluid dynamic control has been studied for the energy flow density in the vicinity of an arc anode. The region in the vicinity of an arc anode has been utilized as a high-energy source. A constricting gas flow is capable of generating an extra fine arc, so-called "point arc" [1]. Cool inert gas is blown centripetally and spirally against the anode spot and forms the constricting gas flow.

The blowing gas is also capable of controlling the heat flux distribution on a transferred anode [2]. The radial inward flow or the vortex flow is blown from the circumference to the transferred arc. The heat flux distribution on the anode has been measured, and the fluid dynamic control has been investigated experimentally.

The purpose of this paper is to estimate the ability in control of the heat flux distribution on a transferred anode by use of a blowing gas. The numerical simulation is performed for the anode region of the transferred arc controlled by the blowing

gas. The two-dimensional continuity, x-, r- and θ -momentum, energy and current continuity equations are solved simultaneously with SIMPLER algorithm. The effects of the blowing gas on the heat transfer distribution are investigated numerically.

2. NUMERICAL FORMULATION

2.1 Basic Model and Assumption

The model of the arc under atmospheric pressure is shown in Fig. 1. The arc is struck between a conical water-cooled tungsten cathode and a flat water-cooled copper anode. The arc is constricted by a water-cooled nozzle of 8 mm I.D. which floats electrically. The flow rate of argon plasma gas is 10 or 12.5 litre/min. The arc current is 100 A.

The following assumptions are made:

- Steady-state laminar flow.
- Local thermodynamic equilibrium.
- Axially symmetric.
- Optically thin.
- Negligible viscous dissipation and gravity force.

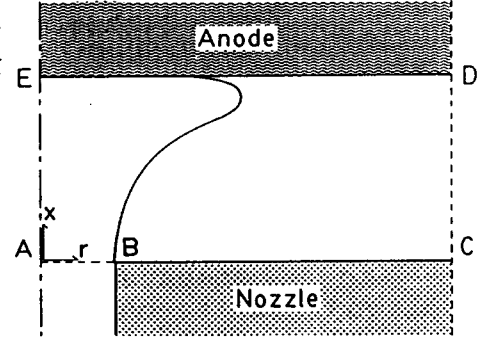


Fig. 1 Calculation model.

2.2 Governing Equations and Boundary Conditions

The governing equations are formulated in the cylindrical coordinate.

Continuity:

$$\frac{1}{r} \cdot \frac{\partial}{\partial r} (r \rho v) + \frac{\partial}{\partial x} (\rho u) = 0 \quad (1)$$

where ρ is the mass density, and u and v are the axial and radial velocity, respectively.

Momentum:

$$\rho \left(u \frac{\partial u}{\partial x} + v \frac{\partial u}{\partial r} \right) = -\frac{\partial p}{\partial x} + 2 \frac{\partial}{\partial x} \left(\mu \frac{\partial u}{\partial x} \right) + \frac{1}{r} \cdot \frac{\partial}{\partial r} \left[\mu r \left(\frac{\partial u}{\partial r} + \frac{\partial v}{\partial x} \right) \right] + j_r B_\theta \quad (2)$$

$$\rho \left(u \frac{\partial v}{\partial x} + v \frac{\partial v}{\partial r} \right) = -\frac{\partial p}{\partial r} + 2 \frac{\partial}{\partial r} \left(\mu r \frac{\partial v}{\partial r} \right) + \frac{\partial}{\partial x} \left[\mu \left(\frac{\partial u}{\partial r} + \frac{\partial v}{\partial x} \right) \right] - \frac{2 \mu v}{r^2} + \frac{\rho w^2}{r} - j_x B_\theta \quad (3)$$

$$\rho \left(u \frac{\partial w}{\partial x} + v \frac{\partial w}{\partial r} \right) = \frac{1}{r} \cdot \frac{\partial}{\partial r} \left[\mu r^2 \frac{\partial}{\partial r} \left(\frac{w}{r} \right) \right] + \mu \frac{\partial}{\partial r} \left(\frac{w}{r} \right) + \frac{\partial}{\partial x} \left(\mu \frac{\partial w}{\partial x} \right) + \frac{\rho v w}{r} \quad (4)$$

where w , p , μ , j_r , j_x , and B_θ are the azimuthal velocity, the pressure, the viscosity, the radial and the axial current density, and the self-induced magnetic field, respectively.

Energy:

$$\rho \left(u \frac{\partial h}{\partial x} + v \frac{\partial h}{\partial r} \right) = \frac{1}{r} \cdot \frac{\partial}{\partial r} \left(r \frac{k}{C_p} \cdot \frac{\partial h}{\partial r} \right) + \frac{\partial}{\partial x} \left(\frac{k}{C_p} \cdot \frac{\partial h}{\partial x} \right) + \frac{j_r^2 + j_x^2}{\sigma} + \frac{5 k_B}{2 e} \left(j_r \frac{1}{C_p} \cdot \frac{\partial h}{\partial r} + j_x \frac{1}{C_p} \cdot \frac{\partial h}{\partial x} \right) \quad (5)$$

where h is the enthalpy, C_p is the specific heat at constant pressure, k is the thermal conductivity, σ is the electrical conductivity, k_B is the Boltzmann constant, and e is the elementary charge.

Current continuity:
$$\frac{1}{r} \cdot \frac{\partial}{\partial r} (r j_r) + \frac{\partial}{\partial x} (j_x) = 0 \quad (6)$$

The last terms in the right hand in Eqs. (2) and (3) represent the terms due to the Lorentz force. The self-induced magnetic field is required in these terms, and it is written as follows:

$$B_\theta = \frac{\mu_0}{r} \int_0^r j_x \xi \, d\xi \quad (7)$$

where μ_0 is the permeability of vacuum.

The calculation domain (ABCDEA) is shown in Fig. 1. The distributions of temperature, velocity and current density at the nozzle exit (AB) are taken from the experimental values. At the line BC which floats electrically, no-slip condition is employed. At the boundary CD, the streamlines are assumed to be perpendicular to the line CD, and the no-current flow and the atmospheric pressure are imposed. The boundary CD is 30 mm away from the arc axis. At the line DE, the temperature is assumed to be 1000 K, and no-slip condition is postulated. At the centerline EA, symmetry conditions are employed. The distance between the nozzle exit and the anode surface is kept at 10 mm.

2.3 Calculation Procedure

The governing equations (1)-(6) are solved using SIMPLER algorithm [3]. The calculations are performed for a nonuniform grid system of 15 x 17 in the radial and axial directions, respectively.

The heat flux distribution on the anode is estimated from the calculated distributions of the velocity, the temperature and the current density. The four mechanisms of the heat transfer on the anode are considered in this study as follows; Q_{conv} : heat transfer by convection, Q_{elec} : heat transfer caused by the electron enthalpy flux, Q_{work} : heat transfer caused by the anode work function, and Q_{fall} : heat transfer caused by electrons accelerated in the anode fall.

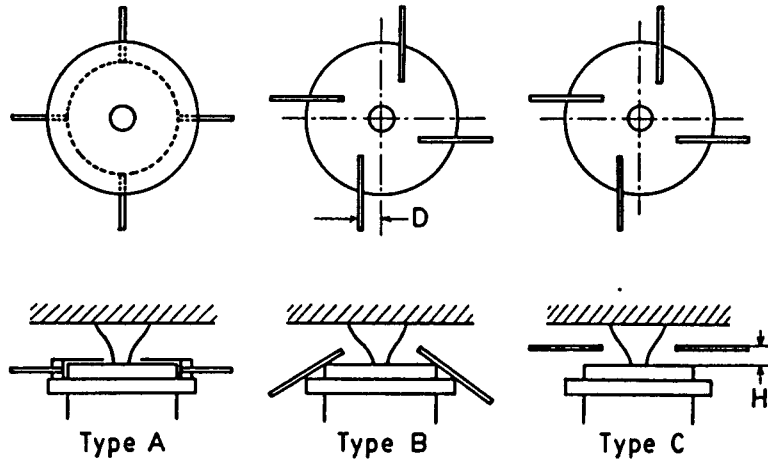


Fig. 2 Top and side views of blowing devices.

3. RESULTS AND DISCUSSION

Computations are performed for a transferred arc under atmospheric pressure with a blowing gas. Argon (300 K) is used as the blowing gas with three types (type A, B or C) as shown in Fig. 2. A radial inward flow is blown at the nozzle exit with the type A. A vortex flow is blown with the type B or C. The blowing gas is injected tangentially toward the anode spot with the type B, and is injected horizontally and tangentially with the type C. Figure 2 also illustrates the blowing position (offcentered distance: D , and the height: H). For the type B, $D=5$ mm and $H=5$ mm; for the type C, $D=5$ mm and $H=3$ mm.

Figure 3 represents the radial distribution of the heat flux on the anode, due to the various mechanisms, without the blowing (plasma gas flow rate: 12.5 litre/min). The energy flux caused by electrons entering the anode, Q_{work} , Q_{fall} and Q_{elec} , plays a significant role in the heat transfer mechanism in the vicinity of the center. At the center, Q_{work} and Q_{fall} contribute 42 % and 36 % to the heat flux, respectively. In the arc fringe, Q_{conv} is dominant to the heat flux because of the broad distribution of the temperature and the sharp distribution of the current density on the anode.

Figure 4 demonstrates the calculated heat flow within a five-millimeter radius of the anode center with the blowing type A. The large heat flow in this figure indicates the sharp distribution of the heat transfer on the anode. The heat transfer distribution is broadened with the blowing gas at small flow rates. The distribution is, however, sharpened gradually with increasing flow rate of the blowing gas above 10 litre/min. The distribution of the total heat flux is mainly dependent on the distribution of Q_{work} and Q_{fall} because the sum of Q_{work} and Q_{fall} contributes approximately 80 % to the total heat flow within a five-millimeter radius of the anode center.

The heat transfer distribution

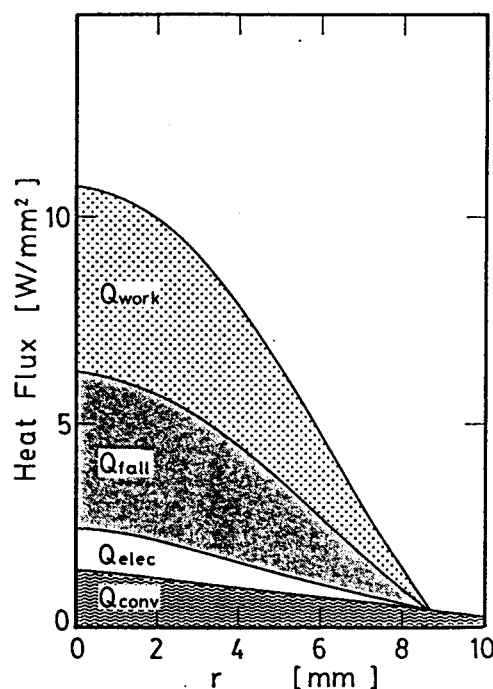


Fig. 3 Radial distributions of heat flux on the anode without blowing. (Plasma gas: 12.5 litre/min)

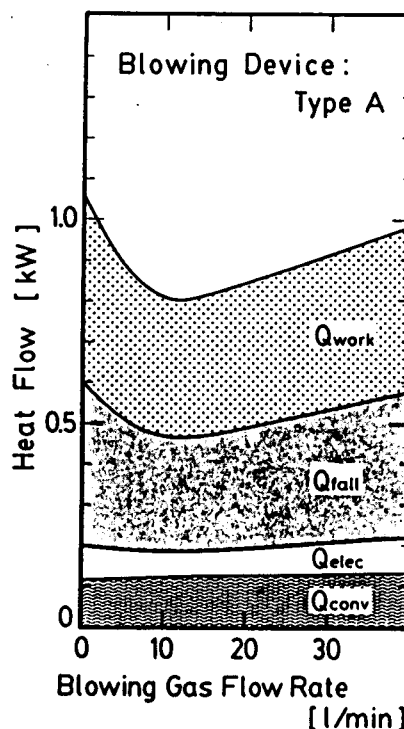


Fig. 4 Effect of blowing gas flow rate with Type A. (Plasma gas: 10 litre/min)

is chiefly controlled by the distribution of the current density. The radial distributions of the axial current density are shown in Fig. 5. The arc is constricted by the blowing gas at a flow rate of 10 litre/min at the blowing position ($x=1.0$ mm), but is broadened near the anode surface ($x=9.75$ mm). The constricted arc at the nozzle exit leads to a large velocity of the arc, and to the wide arc on the anode. The arc current density near the anode is slightly increased by the blowing gas at a flow rate of 30 litre/min. The large flow of the blowing gas cools the arc periphery on the anode and brings about the slightly sharp distribution of the heat transfer.

The heat flow on the anode with the blowing type B is presented in Fig. 6. The heat flux is sharpened with an increase in the blowing gas velocity. The distribution reaches the limit at the blowing velocity of 20 m/s because the arc on the anode is cooled at a velocity above 20 m/s.

The distribution of the axial velocity and the temperature near the blowing position are shown in Fig. 7. These distributions, especially in the arc fringe, are constricted by the blowing gas. The vortex flow of the blowing gas toward the anode spot forms the sharp distribution of the energy flow of the arc. The distributions of the arc pressure and the axial current density in Fig. 8 also indicate the effects of the blowing gas.

Figure 9 represents the heat flow at the anode with the blowing type C. This figure shows the similar results to those with the type B. The distributions of the axial velocity, the temperature, the arc pressure and the axial current density are also similar to those with the type B. The vortex flow injected horizontally is able to sharpen the heat flux distribution on the anode.

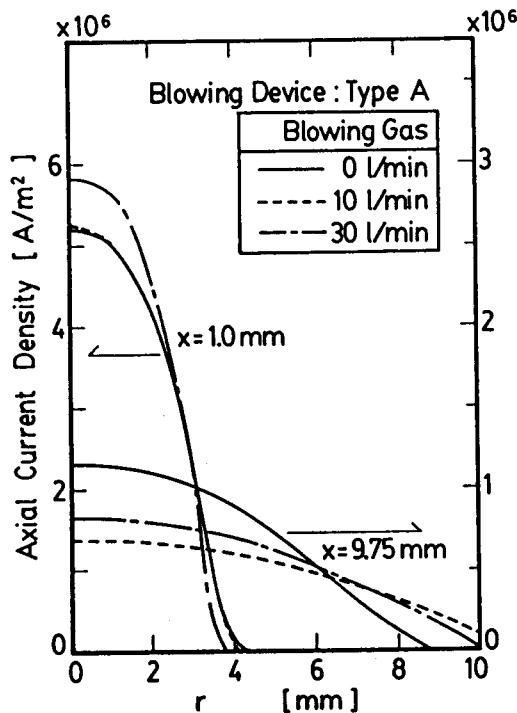


Fig. 5 Radial distributions of axial current density with type A. (Plasma gas: 10 litre/min)

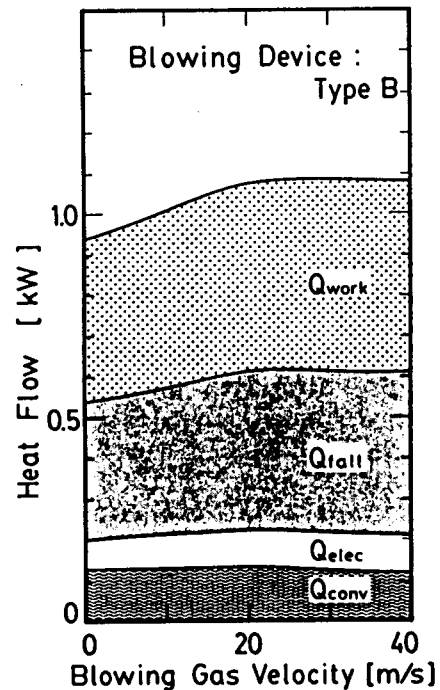


Fig. 6 Effect of blowing gas velocity with type B. (Plasma gas: 12.5 litre/min)

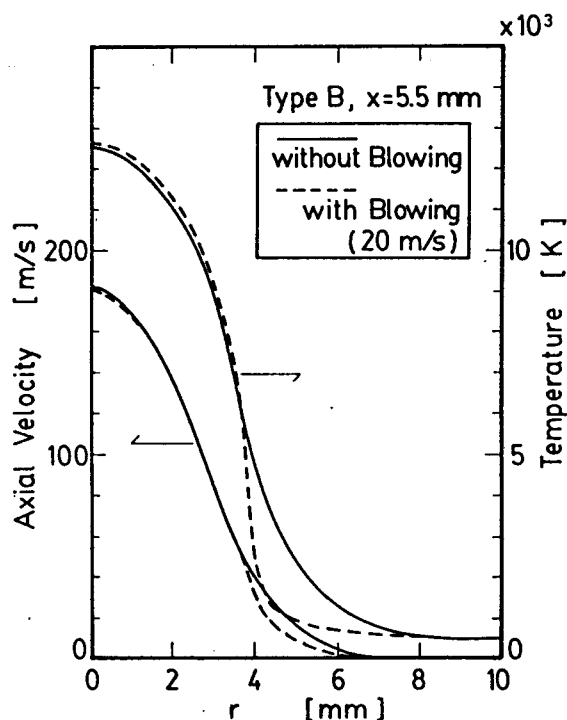


Fig. 7 Radial distributions of axial velocity and temperature with type B.
(Plasma gas: 12.5 litre/min)

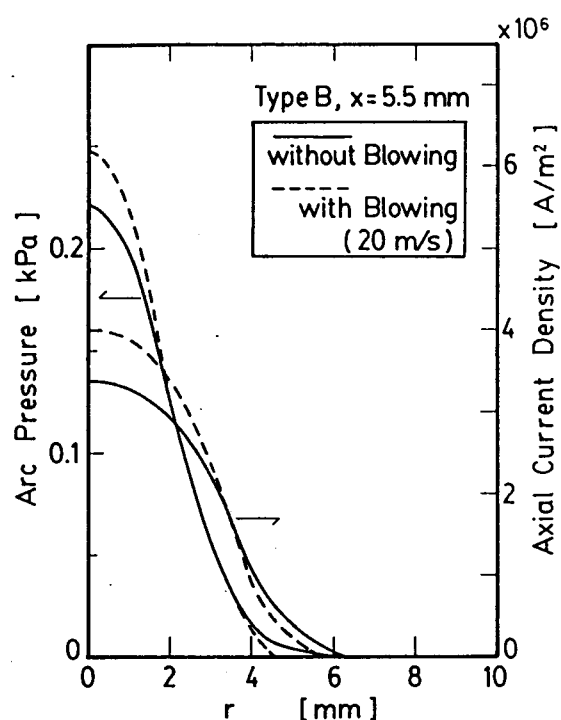


Fig. 8 Radial distributions of arc pressure and axial current density with type B.
(Plasma gas: 12.5 litre/min)

4. CONCLUSIONS

Fluid dynamic control of an arc has been investigated numerically. The heat transfer distribution at the transferred anode is sharpen by the vortex flow of the blowing gas. The distribution is broaden by the radial inward flow blown at the nozzle exit.

REFERENCES

- [1] Y.Arata and K.Inoue, Trans. JWRI, 3 (1974) 201.
- [2] T.Watanabe, K.Nagashima, T.Honda and A.Kanzawa, J. High Temp. Soc. Japan, 16 (1990) 83.
- [3] S.V.Patanker, Numerical Heat Transfer and Fluid Flow, McGraw-Hill, New York (1980).

ACKNOWLEDGMENT

This work was supported by the Amada Foundation for Metal Work Technology.

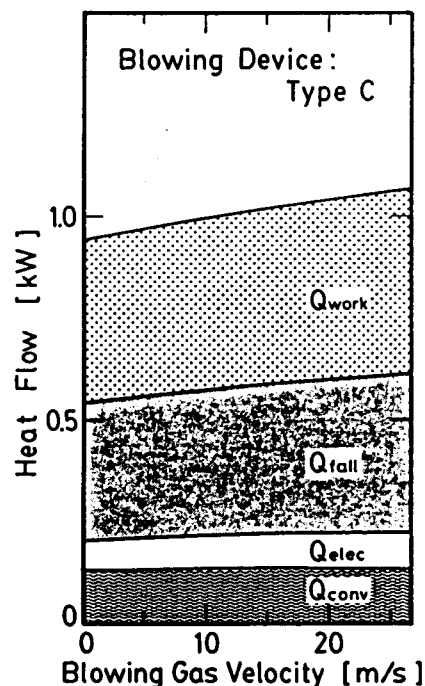


Fig. 9 Effect of blowing gas velocity with type C.
(Plasma gas: 12.5 litre/min)